

1 **RLINE: A Line Source Dispersion Model for Near-Surface Releases**

2 Michelle G. Snyder^{1*}, Akula Venkatram², David K. Heist¹, Steven G. Perry¹,
3 William B. Petersen³, Vlad Isakov¹

4 ¹ U.S. Environmental Protection Agency, Office of Research and Development, National
5 Exposure Research Laboratory, Atmospheric Modeling and Analysis Division, Research
6 Triangle Park, NC 27711 USA

7 ²University of California, Riverside, CA 92521

8 ³William B. Petersen, Consulting, Research Triangle Park, NC

9
10
11
12
13
14
15
16
17
18
19
20
21
22
23
24
25
26
27
28
29
30 *corresponding author: Michelle G. Snyder (Snyder.Michelle@epa.gov)

31 **ABSTRACT**

32 This paper describes the formulation and evaluation of RLINE, a Research LINE source
33 model for near-surface releases. The model is designed to simulate mobile source pollutant
34 dispersion to support the assessment of human exposures in near-roadway environments
35 where a significant portion of the population spends time. The model uses an efficient
36 numerical integration scheme to integrate the contributions of point sources used to represent
37 a line-source. Emphasis has been placed on estimates of concentrations very near to the
38 source line. The near-surface dispersion algorithms are based on new formulations of
39 horizontal and vertical dispersion within the atmospheric surface layer, details of which are
40 described in a companion paper (Venkatram et al. 2013), This paper describes the general
41 formulations of the RLINE model, the meteorological inputs for the model, the numerical
42 integration techniques, the handling of receptors close to the line source, and the performance
43 of the model against developmental data bases and near-road concentrations from
44 independent field studies conducted along actual highway segments.

45 **KEYWORDS**

46 *Near-surface dispersion, near-road concentrations, surface releases, similarity theory,*
47 *meteorological measurements, urban dispersion, Idaho Falls experiment, RLINE*

48 **1 Introduction**

49 Growing concern about human exposure and related adverse health effects near roadways
50 motivated an effort by the U. S. Environmental Protection Agency to reexamine the
51 dispersion of mobile source related pollutants. Studies have shown that living near roadways
52 is implicated in adverse health effects including respiratory problems (e.g. McCreanor et al.
53 2007), birth and developmental defects (Wilhelm and Ritz 2003), premature mortality (e.g.
54 Krewski et al. 2009), cardiovascular effects (Peters et al. 2004; Riediker et al. 2004) and
55 cancer (Harrison et al. 1999; Pearson et al. 2000). These studies of traffic-related health
56 effects have included both short-term (e.g., hourly) and long-term (e.g., annual) exposures.
57 (Krewski et al. 2009; McCreanor et al. 2007)

58 Estimating exposure to roadway emissions requires dispersion modeling to capture the
59 temporal and spatial variability of mobile source pollutants in the near-road environment. The
60 model needs to account for the variability in mobile emissions across a myriad of urban and
61 suburban landscapes, while considering factors (depending on pollutant and application
62 scenario) such as vehicle induced turbulence, roadway configurations (e.g. depressed
63 roadways and noise barriers), local meteorology, surrounding terrain and buildings, pollutant
64 chemistry, deposition, and others.

65 There are several models in the literature that have been developed to simulate dispersion
66 from roadways. Examples include HIWAY-2 (Petersen 1980), UCD (Held et al. 2003), CAR-
67 FMI (Harkonen et al. 1995), GM (Chock 1978), OSPM (Hertel and Berkowicz 1989),
68 ADMS-ROADS (McHugh et al. 1997), CFD-VIT-RIT (Wang and Zhang 2009) and the
69 CALINE series of models (Benson 1989, 1992). Because urban areas typically contain a
70 large number of road segments, computational efficiency is an important factor in
71 formulating a line source dispersion model. As a result, most models for dispersion of
72 roadway emissions are analytical approximations to the integral associated with modeling a
73 line source as a set of point sources. However, these approximations can lead to large errors
74 when the winds are light and variable, when the wind direction is close to parallel to the road

75 and when the source and receptor are at different heights (Briant et al, 2011). So the current
76 version of RLINE is based on Romberg numerical integration of the contributions of point
77 sources along a line (road segment). This approach allows us to incorporate the governing
78 processes without introducing errors associated with approximating the underlying model
79 framework.

80 The point contributions along the line source are computed with the Gaussian, steady-state
81 plume formulation. This is consistent with models currently recommended by the U. S. EPA
82 for regulatory applications e.g. CALINE3 (Benson 1992) and AERMOD (Cimorelli et al.
83 2005).

84 RLINE is designed to simulate primary, chemically inert pollutants with emphasis on near
85 surface releases and near source dispersion. The model has several features that distinguishes
86 it from other models. It includes new formulations for the vertical and horizontal plume
87 spread of near surface releases based on historical field data (Prairie Grass, Barad, 1958) as
88 well as a recent tracer field study (Finn et al. 2010) and recent wind tunnel studies (Heist et
89 al. 2009). Details of the formulations are found in the companion paper by Venkatram
90 (2013). Additionally, the model contains a wind meander algorithm that accounts for
91 dispersion in all directions during light and variable winds. To facilitate application of the
92 model, its meteorological inputs are consistent with those used by the AERMOD model
93 (Cimorelli et al., 2005). In addition to evaluation against the Finn et al., 2010 tracer data, the
94 model has been compared with measurements from two independent field studies performed
95 along actual highway segments covering a wide range of meteorological conditions (Baldauf
96 et al. 2008; Benson 1989). The current version of RLINE applies for flat roadways.
97 However, the model framework is designed to facilitate the inclusion of algorithms for
98 depressed roadways and roadways with noise barrier. These complex roadway algorithms
99 will be included in a near future version of the model.

100 This paper describes the general formulations of the RLINE model including new horizontal
101 and dispersion formulations. the handling of receptors very close to the source, and the
102 meteorological inputs for the model. Then, we evaluate performance of the model against
103 both a developmental data base and near-road concentrations from two independent field
104 studies

105 **2 The Line Source Model**

106 The concentration from a finite line source in RLINE is found by approximating the line as a
107 series of point sources. The number of points needed for convergence to the proper solution is
108 determined by the model and, in particular, is a function of distance from the source line to
109 the receptor. Each point source is simulated using a Gaussian plume formulation. Here we
110 explain the implementation of the point source plume model and the integration scheme used
111 to approximate a line source. We begin with a description of the meteorological inputs
112 needed for the model.

113 **2.1 Meteorological Inputs**

114 The meteorology that drives RLINE is obtained from the surface file output from
115 AERMOD's met processor, AERMET (Cimorelli et al. 2005). AERMET processes surface
116 characteristics (surface roughness, moisture and albedo), cloud cover, upper air temperature
117 soundings, near surface wind speed, wind direction and temperature to compute the surface
118 variables needed by AERMOD. The specific variables that are needed by RLINE include,

119 the surface friction velocity (u_*), the convective velocity scale (w_*), Monin-Obukhov length
 120 (L), the surface roughness height (z_0), and the wind speed and direction at a reference height
 121 within the surface layer.

122 Additionally, for light wind, stable conditions, when u_* is generally small, an adjustment is
 123 made to the friction velocity based on the work of (Qian and Venkatram 2011). From an
 124 examination of stable periods within meteorological field measurements collected in
 125 Cardington, Bedfordshire as wind speeds became small Qian and Venkatram found that u_*
 126 was much larger than values predicted by those from AERMET. From the formulations in
 127 AERMET and assuming a constant value of the temperature scale, $T_* = \frac{\overline{w'T'}}{u_*} = 0.08$, where
 128 $\overline{w'T'}$ is the mean vertical temperature flux, u_* takes the form

$$u_* = \frac{C_{DN}^{1/2} U_r}{2} [1 + (1 - r^2)^{1/2}] \quad (1)$$

129 where

$$C_{DN} = \frac{\kappa^2}{\left(\ln\left(\frac{z_r - d_h}{z_0}\right)\right)^2}, \quad (2)$$

130

$$r = \frac{U_{crit}}{U_r}, \quad (3)$$

131

$$U_{crit} = \frac{2u_0}{C_{DN}^{1/4}}, \quad (4)$$

132 and

$$u_0 = \left(\frac{\beta g(z_r - d_h - z_0)T_*}{T_0}\right)^{1/2} \quad (5)$$

133 where d_h is the canopy displacement height, κ the von karman constant, U_r is the wind speed
 134 measured at the reference height, z_r and T_0 is the temperature at reference height.

135 Qian and Venkatram recommend the following modification to Eqn. 22 for cases of light
 136 winds (low u_*) and stable atmospheric conditions ($L > 0$)

$$u_* = \frac{C_{DN}^{1/2} U_r}{2} \left[\frac{1 + \exp(-r^2/2)}{1 - \exp(-2/r)} \right] \quad (6)$$

137 Once u_* has been adjusted for light wind, then L and all other parameters affected by this
 138 adjustment are recalculated using the AERMET methodology for internal consistency.

139 RLINE has a lower limit for the effective wind speed used in the dispersion calculations that
 140 is a function of the lateral turbulence. The horizontal wind energy is composed of a mean

141 component u^2 and two random wind energy components, σ_u^2 and σ_v^2 . Assuming these
 142 random components to be approximately equal, when the mean wind goes to zero, the
 143 horizontal wind energy will maintain at $2\sigma_v^2$. Therefore, the minimum effective wind speed is
 144 set at $\sqrt{2} \cdot \sigma_v$. From (Cimorelli et al. 2005), the lateral turbulent wind component is
 145 computed as

$$\sigma_v = \sqrt{(0.6w_*)^2 + (1.9u_*)^2} \quad (7)$$

146 where w_* is the convective velocity scale.

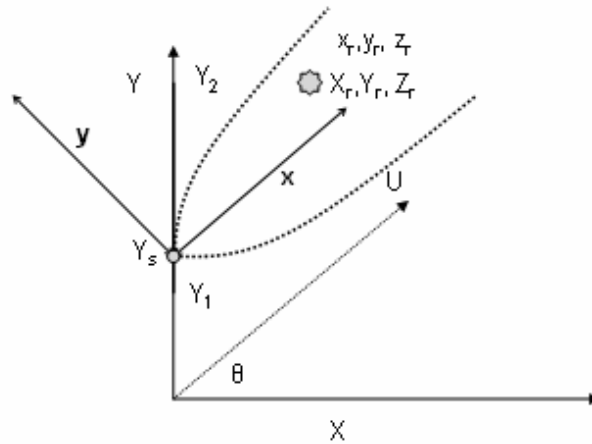
147 Therefore, the effective wind speed is:

$$U_e = \sqrt{2\sigma_v^2 + U(\bar{z})^2}. \quad (8)$$

148 Here the wind speed, U , is evaluated at the mean plume height, \bar{z} . The mean plume height
 149 depends on the vertical spread of the Gaussian plume, which will be described in section
 150 2.3.1.

151 2.2 Numerical line source approximation

152 The mathematical formulation to compute the impact of a line source is simplified by using a
 153 coordinate system where the Y -axis lies along the line source as shown in Figure 1. The wind
 154 direction is oriented at an angle, θ , relative to the X -axis, and the receptor coordinates are given
 155 by (X_r, Y_r, Z_r) .



156

157 **Figure 1: Co-ordinate systems used to calculate contribution of point source at Y_s to**
 158 **concentration at (X_r, Y_r, Z_r) . The system x - y has the x -axis along the mean wind**
 159 **direction, which is at an angle θ to the fixed X axis. The dotted line is a representation**
 160 **of the plume.**

161 If L is the length of the source, $Y_2 = Y_1 + L$. To calculate the concentration at a receptor (X_r, Y_r, Z_r)
 162 caused by emissions from the line source characterized by an emission rate of q
 163 (mass/(time*length)), we represent the line source by a set of point sources of strength $q \cdot dY$
 164 along the line $Y_1 Y_2$.

165 The contribution of the plume originating at Y_s to the receptor concentration is most
 166 conveniently expressed in a co-ordinate system, x - y , with its origin at $(0, Y_s)$, and the x -axis
 167 along the direction of the mean wind; the x -axis is rotated by an angle θ relative to the fixed X -
 168 axis.

169 The horizontal co-ordinates of the receptor in the along-wind coordinate system, (x_r, y_r, z_r) , can
 170 be expressed as

$$\begin{aligned} x_r &= X_r \cos \theta + (Y_r - Y_s) \sin \theta \\ y_r &= (Y_r - Y_s) \cos \theta - X_r \sin \theta \end{aligned} \quad (9)$$

171 The vertical coordinate remains unchanged so that $z_r = Z_r$.

172 Then, the concentration at (x_r, y_r) due to the line becomes

$$C(x_r, y_r) = \int_{Y_1}^{Y_1+L} dC_{pt}, \quad (10)$$

173 where dC_{pt} is the contribution from an elemental point source.

174 The point-source Gaussian plume formulation is the sum of plume components (horizontal
 175 and vertical with subscript pl) and meandering contributions (with subscript m). The plume
 176 component centerline follows the wind direction, as in Figure 1, and the meandering
 177 component, accounting for the random component of the wind, spreads the plume material
 178 radially outward from the source equally in all directions. The two components are added
 179 using a weighting factor, f , based on the magnitudes of the lateral turbulence and the mean
 180 wind.

$$dC_{pt} = (1 - f) \cdot dC_{pl} + f \cdot dC_m \quad (11)$$

where

$$f = \frac{2 \cdot \sigma_v^2}{U_e^2} \quad (12)$$

181 Because U_e has a minimum value of $2\sigma_v$, f is limited to between 0 and 1.

182 The plume concentration is broken into the vertical and horizontal components,

$$dC_{pl} = \frac{qdY_s}{U_e} [VERT \cdot HORZ_{pl}], \quad (13)$$

183 where q is the emission rate.

184 The meander component is given by

$$dC_m = \frac{qdY_s}{U_e} [VERT \cdot HORZ_m] \quad (14)$$

185 The vertical component of the plume and meander concentrations is found by

$$VERT = \frac{1}{\sqrt{2\pi}\sigma_z} \cdot \left[\exp\left(-\frac{1}{2}\left(\frac{z_s - z_r}{\sigma_z}\right)^2\right) + \exp\left(-\frac{1}{2}\left(\frac{z_s + z_r}{\sigma_z}\right)^2\right) \right], \quad (15)$$

186 where the vertical spread, σ_z , will be described in section 2.3.1.

187 The horizontal plume component is found by

$$HORZ_{pl} = \frac{1}{\sqrt{2\pi}\sigma_y} \exp\left(-\frac{1}{2}\left(\frac{y_r - y_s}{\sigma_y}\right)^2\right), \quad (16)$$

188 where the horizontal spread, σ_y , will be described in section 2.3.2.

189 Under low wind speeds, horizontal meander tends to spread the plume over large azimuth
 190 angles, which might even lead to concentrations upwind relative to the vector averaged wind
 191 direction. Adopting the approach in Cimorelli et al. (2005) we assume that as the wind speed
 192 approaches zero, the horizontal plume spreads equally in all directions. Thus the horizontal
 193 meander component in Equation (15) has the form

$$HORZ_m = \frac{1}{2 \cdot \pi \cdot R} \quad (17)$$

$$R = \sqrt{(x_r - x_s)^2 + (y_r - y_s)^2}$$

194 In the Gaussian point source formulation the concentration goes to infinity as the distance
 195 between the source and the receptor goes to zero (since σ_y and σ_z also go to zero). Therefore,
 196 for receptors very near the source, the model sets the minimum distance (along the wind
 197 direction) between the receptor and the line source to one-meter.

198 **2.3 New dispersion formulations**

199 Near surface dispersion has been studied extensively since the 1950s. The Prairie Grass
 200 experiment (PG) (Barad 1958), provided a comprehensive data base that has been used by
 201 several authors to formulate dispersion models for near surface releases (e.g. Briggs 1982;
 202 van Ulden 1978; Venkatram 1992). A new tracer study (Finn et al. 2010) examining
 203 dispersion from a near surface line release provided an opportunity to re-examine the
 204 formulations of σ_z and σ_y in Equations (16) and (17). The companion paper (Venkatram et
 205 al. 2013) provides a detailed reformulation of the dispersion parameters. The resultant
 206 formula incorporated into RLINE are included here.

207 **2.3.1 Vertical Spread**

208 The starting point of the vertical spread reformulation is the solution of the eddy diffusivity
 209 based mass conservation equation proposed by van Ulden (1978). Venkatram et al. (2013)
 210 proposes an interpolation between the limits of very stable and neutral conditions to establish
 211 a relationship between the mean plume height, \bar{z} , and the vertical plume spread, σ_z . In stable
 212 conditions, the vertical spread is given by

$$\sigma_z = a \frac{u_*}{U_e} x \frac{1}{\left(1 + b_s \frac{u_*}{U_e} \left(\frac{x}{L}\right)^{2/3}\right)}, \quad (18)$$

213 where the constants, a and b_s , are obtained empirically. Similarly, for unstable conditions the
 214 vertical spread is found to be

$$\sigma_z = a \frac{u_*}{U_e} x \left(1 + b_u \left(\frac{u_*}{U_e} \frac{x}{L}\right)\right). \quad (19)$$

215 where b_u is an empirical constant for unstable conditions. Note that these expressions for σ_z
 216 are implicit because the wind speed, U_e , on the right hand side of the equation is a function

217 of \bar{z} , which in turn is a function of σ_z . Note also that the expressions for stable (Equation 18)
 218 and unstable (Equation 19) conditions reduce to the same neutral limit for large L.

219 Based on the evaluation of Equations (18) and (19) against the Prairie Grass and the Idaho Falls
 220 tracer experiments, Venkatram et al. (2013) find the following best fit to the coefficients: $a =$
 221 0.57 , $b_s = 3$, and $b_u = 1.5$.

222 The mean plume height, where U_e is evaluated (see Equation 8), is found to be a function of
 223 the vertical spread (Venkatram et al. 2013), and has the form:

$$\bar{z} = \sigma_z \sqrt{\frac{2}{\pi}} \exp\left[-\frac{1}{2}\left(\frac{z_s}{\sigma_z}\right)^2\right] + z_s \operatorname{erf}\left(\frac{z_s}{\sqrt{2}\sigma_z}\right). \quad (20)$$

224 2.3.2 Horizontal Spread

225 Estimates of horizontal dispersion in the surface layer have largely been based on Taylor's
 226 theory (1921) for dispersion in homogeneous turbulence which is based on the Lagrangian
 227 time scale and σ_v . Unfortunately, the plume travel time cannot be defined unambiguously
 228 because the wind speed varies with height. We avoid this problem by using an approach
 229 suggested by Eckman (1994), who showed that the variation of σ_y with distance could be
 230 explained by the variation of the effective transport wind speed, even when the standard
 231 deviation of the horizontal velocity fluctuations is constant with height Venkatram et al.
 232 (2013) use Eckman's equation to derive expressions such that

$$\sigma_y = c \frac{\sigma_v}{u_*} \sigma_z \left(1 + d_s \frac{\sigma_z}{|L|}\right), \text{ for stable conditions} \quad (21)$$

233 and

$$\sigma_y = c \frac{\sigma_v}{u_*} \sigma_z \left(1 + d_u \frac{\sigma_z}{|L|}\right)^{-1/2}, \text{ for unstable conditions} \quad (22)$$

234 where c , d_s , and d_u are empirical constants. Based on the evaluation of Equations (21) and
 235 (22) against the Prairie Grass data, the best fit values for the constants are: $c = 1.6$, $d_s = 2.5$,
 236 and $d_u = 1.0$. As with the vertical spread, a detailed discussion of the horizontal spread
 237 formulation is found in Venkatram et al. (2013).

238 2.4 Numerical Computation of Concentration

239 The right hand side of Equation (10) must be integrated numerically because both σ_y and σ_z
 240 depend on x_r , which in turn is a function of the integrating variable Y_s (See Equation (9)).
 241 This is done in RLINE with an efficient Romberg integration scheme (Press et al. 1992).
 242 Convergence of the scheme is assumed when the difference between estimated concentration
 243 is below a user specified error limit (recommended 1×10^{-3}). When multiple sources are
 244 modeled the cumulative concentration is reported, but each source's contribution is calculated
 245 with an accuracy of the user defined limit.

246 In some cases, such as modeling pedestrian or bike-lane exposures it may be necessary to
 247 estimate concentrations within a few meters of the source. When the receptor is close to the
 248 line source and its concentration in the early steps of the integration scheme is dominated by
 249 a single point source or has little or no impact from any point, convergence may occur too
 250 quickly. Therefore a minimum number of iterations, j_{min} , is calculated that prevents this
 251 premature convergence by ensuring that the spacing between the points used to approximate

252 the line source, dr , is smaller than the distance from receptor to the line. Starting from the
 253 fact that for the j^{th} iteration, the number of points representing the line is $2^{j-1} + 1$, we find that:

$$\frac{L}{dr} < 2^{j-1} + 1 \quad (23)$$

$$j_{min} = \left\lceil \frac{\log\left(\frac{2L}{dr \sin \theta} - 2\right)}{\log 2} \right\rceil, \quad (24)$$

254 where L is the length of the line and $dr \sin \theta$ is the perpendicular distance between the
 255 receptor and the line source. The case of receptors very close to the line source is the most
 256 computationally time consuming. The minimum number of iterations, j_{min} , can be large when
 257 the line source is long and the distance, $dr \sin \theta$, becomes small.

258 3 Model Applications

259 Model performance estimates of concentration are compared qualitatively to on-site
 260 measurements made during the two field studies described below with the use of scatter plots.
 261 In addition, model performance is quantified using the performance statistics as described in
 262 Venkatram (2008). The quantitative model performance measures used here are the
 263 geometric mean bias (m_g), the geometric standard deviation (s_g) and the fraction of estimates
 264 within a factor of two of the measured value (fac2). Venkatram's definition of m_g suggests
 265 that a model is over predictive when $m_g < 1$. We have flipped the ratio of observed-to-
 266 predicted concentrations here, so that $m_g > 1$ is indicative of a model over-prediction;
 267 $m_g < 1$ is indicative of a model under-prediction. The geometric mean bias and standard
 268 deviation are found by:

269

$$m_g = \text{median}\left(\frac{C_p}{C_o}\right) \quad (25)$$

270

$$s_g = \exp\left(\frac{\ln(F)}{\sqrt{2} \text{erf}^{-1}(A_F)}\right), \quad (26)$$

271 where C is the concentration, either observed (subscript 'o') or predicted (subscript 'p'), F is
 272 taken to be 2, A_F is the fraction of the ratio, $C_p/(C_o m_g)$, between $1/F$ and F , and erf^{-1} is the
 273 inverse error function. Observed and predicted concentrations are paired in time and space.

274 3.1 Comparison of Model to Idaho Falls Tracer Study

275 A line source experiment was conducted near Idaho Falls, Idaho in 2008 (Finn et al. 2010).
 276 The study area is located in a broad, relatively flat area on the western edge of the Snake
 277 River Plain. Five tests were conducted during the study, each spanning a 3-h period broken
 278 into 15-min tracer sampling intervals. One test was conducted in unstable conditions, one in

279 neutral conditions, and two in stable conditions; test 4 was not used since the wind shifted
 280 away from the sampler array as the test period began. A brief summary is shown in Table 1.

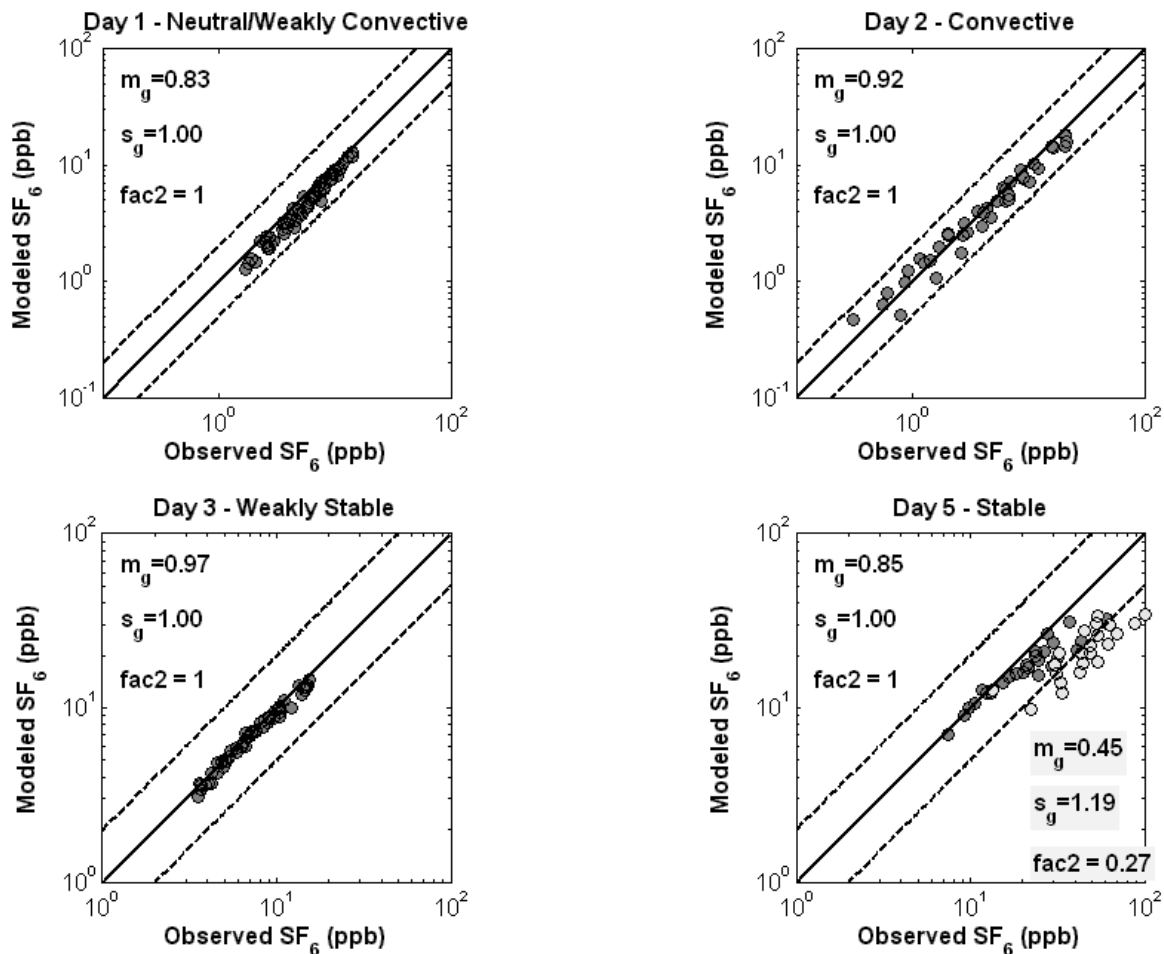
281 **Table 1: Summary of the wind conditions during each day of the Idaho Falls 2008**
 282 **field test.**

Test Day	L (m)	u_* (m/s)	Wind Speed (m/s)	Wind Direction (deg)
1 – Neutral/Weakly Convective	-(500-181.8)	0.52-0.88	5.5-8.1	192.7-228.1
2 - Convective	-(29.8-1.7)	0.15-0.34	0.7-2.5	189-203.9
3 – Weakly Stable	+(35.3-62.0)	0.28-0.35	3.2-3.6	202-208.6
5 - Stable	+(4.9-17.3)	0.05-0.19	1.6-2.4	194.1-230.8

283 The overall purpose of the study was to examine the difference in pollutant dispersion from a
 284 line-source (e.g. roadway) in the presence and in the absence of a 90 meter long and 6 meter
 285 high (H) noise barrier. Simultaneous measurements were made at the barrier and no-barrier
 286 (control) sites. Both sites had a 54 m long SF₆ tracer line source release positioned 1 m
 287 above ground level (AGL). In both experiments, a gridded array of bag samplers were
 288 positioned downwind of the line source for measuring concentrations.

289 Mean wind and turbulence was obtained on the control site from a sonic anemometer within
 290 the sampler array at a 3 meter height. The roughness length scale, z_0 , for the site was
 291 estimated at 0.053 m based on mean wind and sheer stress measurements from the sonic
 292 during the near-neutral conditions of test day 1. In the development and evaluation of RLINE
 293 as described in this paper we have only used the control experiment (non-barrier)
 294 measurements.

295 Figure 2 shows the infinite line source model predications vs. the observed concentrations for
 296 the four cases in Idaho Falls. The infinite line source was constructed from the finite line
 297 measurements using the procedure in Heist et al. (2009).



298

299 **Figure 2: Scatter-plot of the modeled concentration vs. the observed concentration for a**
 300 **crosswind integrated line source during days 1, 2, 3, and 5 of the Idaho Falls 2009 line**
 301 **source field experiment. Grey symbols are for very stable conditions.**

302 The observations on day 5 are split into two groups. The light grey circles indicate periods of
 303 very strong stability. Clearly for these conditions the plume is not well represented by the
 304 model. In the presence of strong convection, the model appears to be overestimating the
 305 vertical spread.

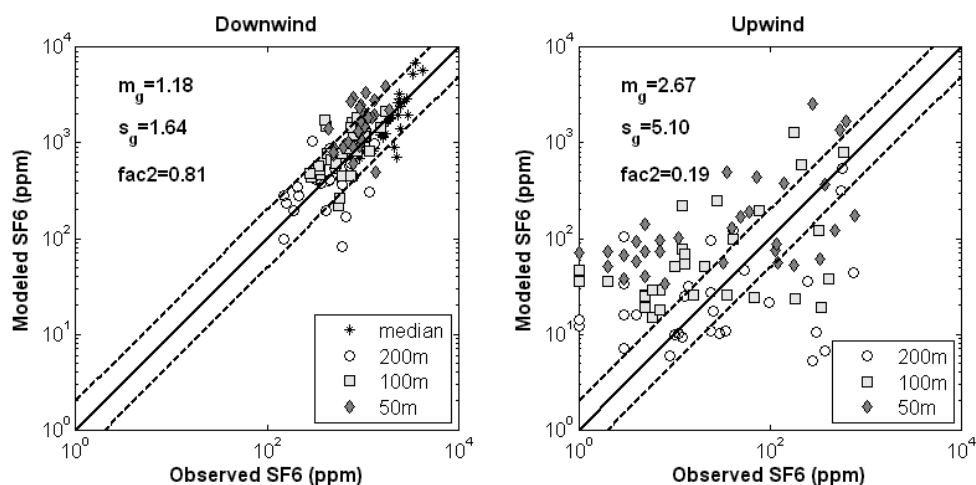
306 3.2 Comparisons to Roadway Measurements

307 Two field study data bases involving free flowing traffic on major highways were selected for
 308 comparison with the RLINE model. The first was a tracer study, CALTRANS Highway 99
 309 (Benson 1989), and the other a study of the dispersion of nitrogen oxide near an interstate
 310 highway, Raleigh 2006 (Baldauf et al. 2008).

311 The CALTRANS Highway 99 Tracer Experiment was conducted in the winter of 1981-1982
 312 along a four kilometer section of U. S. Highway 99 in Sacramento, California. During the
 313 period of the experiment, the highway carried approximately 35,000 vehicles per day. The
 314 surrounding terrain is flat with open fields and parks and scattered residential development.
 315 The experiment location had 2 lanes of traffic northbound and two southbound separated by a
 316 14 m median. Tracer concentration measurements were taken at four locations in the highway
 317 median and at 50, 100, and 200 m distances perpendicular to the roadway in each direction.
 318 Tracer gas, SF_6 , was released through the exhaust system of vehicles at specified intervals as

319 they traveled down each side of the highway to simulate a quasi-continuous line release
320 during the measurement periods. All tracer samples were taken at one meter above the local
321 surface and on site measurements of meteorology were taken from a 12 m tower.

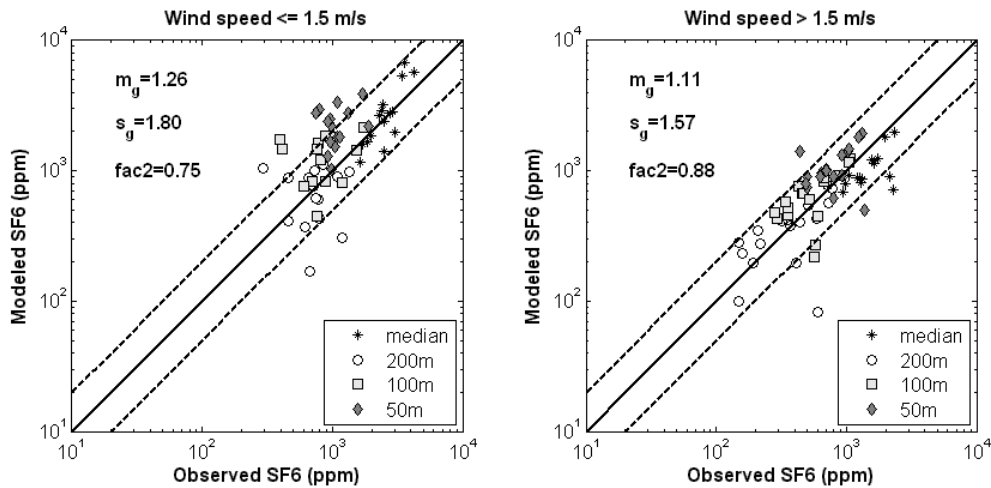
322 Figure 3 shows a comparison of the model estimates to the measurements for cases where the
323 mean wind direction is within 60 degrees of perpendicular to the highway, while
324 distinguishing upwind and downwind concentrations. The model performs well for
325 downwind receptors with over 80% of the estimates within a factor of two of the observations
326 and the geometric mean value showing a slight overprediction at 0.89. The highest
327 observations, not surprisingly, are found at the median locations as are the model estimates.
328 The range of concentrations over all downwind locations for model and observations is
329 approximately the same.



330
331 **Figure 3: Comparison of RLINE modeled concentrations to those measured during**
332 **CALTRANS99 for winds within 60 degrees of perpendicular to Highway 99.**

333 For upwind receptors, the scatter is much larger and the performance reduced. The geometric
334 mean suggests an overprediction by about a factor of two and the geometric standard
335 deviation reveals scatter six times larger than that for downwind receptors. In looking at the
336 distribution of the data points, the observations show no distinguishable trend in
337 concentrations with distance from the highway. The model, however, does display a
338 decreasing trend with distance. This suggests that there may be other factors influencing the
339 observed upwind concentrations that are dominating the expected concentration decay with
340 distance from the line source. One possibility may be small plume rise from a heated
341 highway or from hot exhaust that can have a strong influence on the turbulence driven nature
342 of upwind dispersion. These results suggest that further research into the upwind dispersion
343 algorithm is necessary.

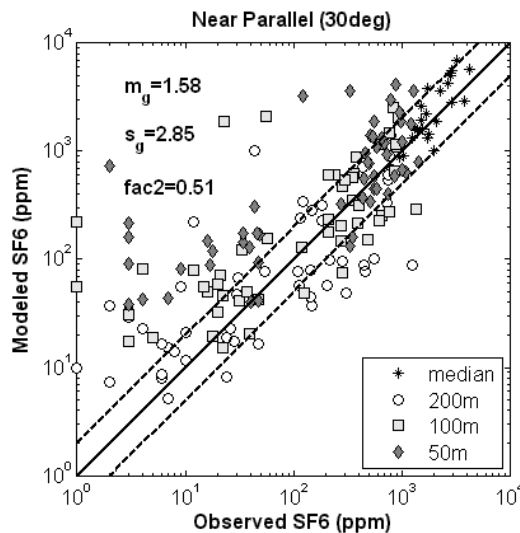
344 Expanding the analysis of the downwind values in Figure 3, the distinction between low and
345 moderate winds is examined. In Figure 4 is displayed the model performance for winds
346 below and above 1.5 ms^{-1} . The values at the median locations match well between model and
347 observations for all wind speeds suggesting that the initial dispersion estimates are good in
348 the model. For moderate to high winds, the model is performing at its best. For light winds,
349 there is a slight degradation of this performance with a slight tendency to overpredict the
350 concentrations particularly at 50 and 100 meters downwind. Light winds are related to more
351 extremes in stability (stable or unstable). Therefore an examination of the dispersion rates for
352 these conditions will be a subject of future work.



353

354 **Figure 4: Expansion of the analysis of the downwind concentration comparisons of**
 355 **Figure 4 based on wind speed.**

356 Figure 5 shows the comparison of model estimates to observations at all sampler locations for
 357 wind direction within 30 degrees of parallel to the highway. Unlike the cases when winds
 358 approach the roadway at an oblique angle, with near parallel winds concentrations become
 359 very sensitive to wind direction. In particular, the formulation of the lateral dispersion
 360 becomes much more important as does the influence of the meander component. Overall, the
 361 model tends to overpredict these conditions by a little less than a factor of two ($m_g = 0.56$),
 362 with half of the estimates within a factor of two of the observations. For the sampler
 363 locations within the median of the highway the model is performing particularly well, which
 364 adds confidence to the emissions and near-source characterization. The tendency toward
 365 overprediction is particularly pronounced for the smaller observed concentrations with a
 366 somewhat better performance for the higher concentrations. Overprediction of the smaller
 367 concentrations, as in Figure 5, represents an overestimation in the upwind concentration. This
 368 outcome suggests that perhaps the meander component may be over estimated.

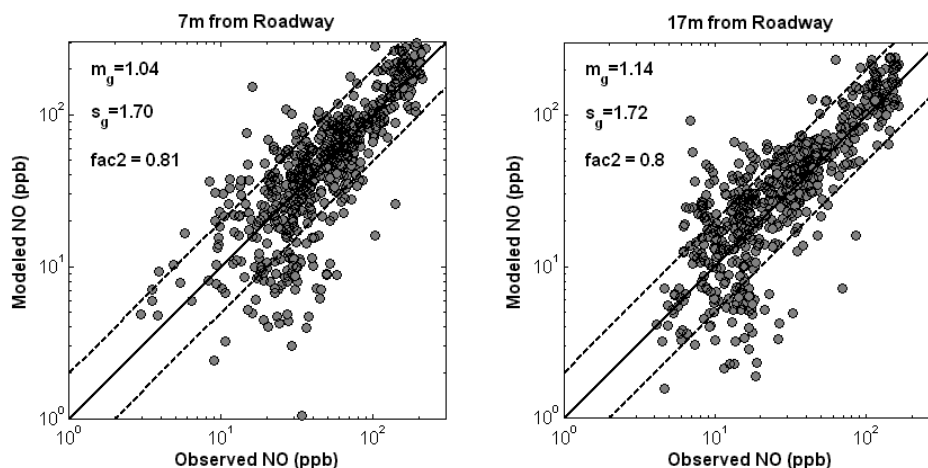


369

370 **Figure 5: Comparison of RLINE modeled concentrations to those measured during**
 371 **CALTRANS99 for wind that were within 30 degrees of parallel to Highway 99.**

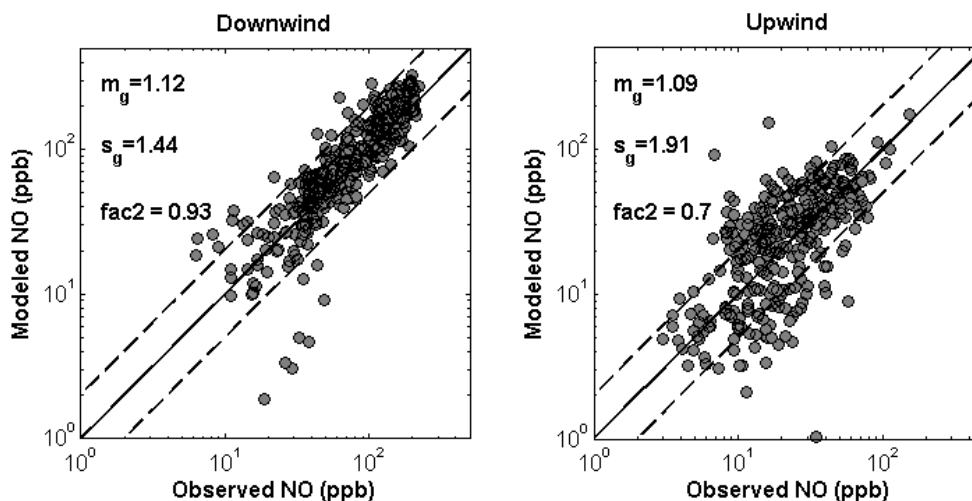
372 In July and August 2006 a roadway study was conducted in Raleigh, NC along a busy section
 373 of I-440 supporting approximately 125,000 vehicles per day (Baldauf et al. 2008). This

374 analysis is based on NO measurements collected at 7 m and 17 m from the roadway shoulder
 375 (at a height of 2 m). Thoma et al (2008) presents nearly identical time-series measurements
 376 NO and NO₂ during this study, thus chemical transformation is negligible in this case. On site
 377 measurements of traffic and meteorology were collected along with NO concentrations. We
 378 used traffic counts from the study and emission factors as found by Venkatram et al. (2007).
 379 Although these emission factors were determined, in part, using dispersion calculations, the
 380 comparisons here are an independent test of RLINE's ability to capture the concentration
 381 distribution as well as the concentration fall off as a function of distance. Model estimates
 382 versus measured concentrations are shown in Figure 6 for the two monitor locations.



383
 384 **Figure 6: Scatter-plot of Raleigh 2006 NO observed concentration versus the RLINE**
 385 **predicted concentration for each NO receptor.**

386 Agreement between model and observations is good as suggested by both the geometric
 387 mean and the percent within a factor of two. This is true for both sampler locations. The
 388 model does show increased scatter for some moderate to low concentrations. Examining the
 389 data further, Figure 7 shows two subsets of the data in Figure 6. On the left is shown the
 390 model to observation comparisons for mean winds within 60 degrees of perpendicular to the
 391 roadway and blowing toward the monitors, i.e. downwind. The right figure shows the same
 392 plus or minus 60 degree sector only with the wind direction away from the monitors, i.e.
 393 upwind. So the increased scatter noted in Figure 7 is, in fact, mostly related to upwind
 394 concentrations where the model is simulating plume meander. For this data base, the model
 395 is performing fairly well, on average, in estimating the upwind concentrations, however the
 396 distribution of modeled concentrations is clearly much wider than that of the observations.
 397 As with the Caltrans 99 data base, there appears to be a need to further examine the meander
 398 algorithm in the model with the goal of reducing the scatter.



399

400 **Figure 7: Scatter-plot of Raleigh 2006 NO observed concentration versus the RLINE**
 401 **predicted concentration for both NO receptors (7 and 17 m); a) receptors are downwind**
 402 **of roadway and b) receptors are upwind of roadway.**

403 **4 Summary**

404 RLINE, a steady-state, line-source dispersion model, has been developed for near-surface
 405 applications with emphasis on simulating impacts from mobile source emissions of primary
 406 air pollutants in near-road environments. A line is simulated as the sum of the contributions
 407 from point sources, the number determined by the model based on the source to receptor
 408 distance and the convergence criteria. Focus has been placed on dispersion within the first
 409 few hundreds meters of the source and for releases within the surface layer and near the
 410 surface. New dispersion approaches have been formulated from theoretical foundations, with
 411 empirical coefficients based on field tracer studies and wind tunnel simulations, and have
 412 been tested within the RLINE model platform against independent roadway field study data
 413 bases. Plume meander and upwind dispersion are simulated by the model. Adjustments to the
 414 atmospheric boundary layer parameters are considered for light wind conditions and lateral
 415 turbulence is considered in keeping the wind speed near the surface from reaching an
 416 unrealistically small value.

417 The RLINE model was evaluated with the line source field study conducted in Idaho Falls in
 418 2008 (Finn et al. 2010). The model compared well for most meteorological conditions with a
 419 tendency to slightly underpredict. All observations are within a factor of two and geometric
 420 mean biases are between 1.04 and 1.21, except for very stable conditions during part of one
 421 day of the study. RLINE was also evaluated with near-roadway measurements taken during a
 422 tracer study (in Sacramento, CA) and a real emissions study (in Raleigh, NC), both of which
 423 were conducted with traffic present on major freeways. Overall, in these studies the model
 424 performed well for receptors downwind of the roadways, with a tendency to slightly
 425 overpredict. The model did not perform as well in light wind conditions and for upwind
 426 receptors, with a tendency to overpredict in these cases.

427 The current version of the model is designed for flat roadways (line sources with no
 428 surrounding complexities), though the model framework can accommodate future algorithms.
 429 Areas of ongoing research are leading to expanded model applicability and development of
 430 algorithms for simulating the near-source effects of complex roadway configurations (in

431 particular, noise barriers, depressed roadways, and roadside vegetation) and accounting for
432 the effects of urban areas on both meteorology and dispersion.

433 **5 Acknowledgements**

434 The authors would like to thank the members of the U. S. EPA near-road program. The
435 authors are grateful to Dr. Valerie Garcia of EPA's National Exposure Research Laboratory,
436 and Dr. Richard Baldauf of the EPA Office of Transportation and Air Quality for their
437 collaboration throughout the model development process. In addition, we are thankful for the
438 laboratory support from Dr. Laurie Brixey.

439 **6 Disclaimer**

440 The United States Environmental Protection Agency through its Office of Research and
441 Development funded and managed the research described here. It has been subjected to
442 Agency's administrative review and approved for publication.

443 **7 REFERENCES**

444 Baldauf, R., Thoma, E., Hays, M., Shores, R., Kinsey, J., Gullett, B., Kimbrough, S., Isakov,
445 V., Long, T., Snow, R., Khlystov, A., Weinstein, J., Chen, F.-L., Seila, R., Olson, D.,
446 Gilmour, I., Cho, S.-H., Watkins, N., Rowley, P., Bang, J., 2008: Traffic and
447 Meteorological Impacts on Near-Road Air Quality: Summary of Methods and Trends
448 from the Raleigh Near-Road Study. *Journal of the Air & Waste Management Association*,
449 **58**, 865-878.

450 Barad, M., 1958: Project Prairie Grass. A field program in diffusion AFRCR-TR-58-235.

451 Benson, P. E., 1989: CALINE4-a Dispersion Model for Predicting Air Pollution
452 Concentration near Roadways. FHWA/CA/TL-84/15, 245 pp.

453 ———, 1992: A review of the development and application of the CALINE3 and 4 models.
454 *Atmospheric Environment. Part B. Urban Atmosphere*, **26**, 379-390.

455 Briggs, G. A., 1982: Similarity forms for ground-source surface-layer diffusion. *Boundary*
456 *Layer Meteorology*, **23**, 489-502.

457 Chock, D. P., 1978: A simple line-source model for dispersion near roadways. *Atmospheric*
458 *Environment*, **12**, 823-829.

459 Cimorelli, A.J., S.G. Perry, A. Venkatram, J.C. Weil, R.J. Paine, R.B. Wilson, R.F. Lee,
460 W.D. Peters, R.W. Brode, 2005: AERMOD: A Dispersion Model for Industrial Source
461 Applications. Part I: General Model Formulation and Boundary Layer Characterization.
462 *Applied Meteorology*, **44**, 682-693.

463 Eckman, R. M., 1994: Re-examination of empirically derived formulas for horizontal
464 diffusion from surface sources. *Atmospheric Environment*, **28**, 265-272.

465 Finn, D., Clawson, K.L., Carter, R.G., Rich, J.D., Eckman, R.M., Perry, S.G., Isakov, V.,
466 Heist, D.K., 2010: Tracer studies to characterize the effects of roadside noise barriers on
467 near-road pollutant dispersion under varying atmospheric stability conditions.
468 *Atmospheric Environment*, **44**, 204-214.

- 469 Harkonen, J., E. Valkonen, J. Kukkonen, E. Rantakrans, L. Jalkanen, K. Lahtinen, 1995: An
470 operational dispersion model for predicting pollution from a road. *International Journal*
471 *of Environment and Pollution*, **5**, 602-610.
- 472 Harrison, R. M., P.-L. Leung, L. Somerville, R. Smith, E. Gilman, 1999: Analysis of
473 incidence of childhood cancer in the West Midlands of the United Kingdom in relation to
474 proximity to main roads and petrol stations. *Occupational Environmental Medicine*, **56**,
475 774-780.
- 476 Heist, D. K., S. G. Perry, and L. A. Brixey, 2009: A wind tunnel study of the effect of
477 roadway configurations on the dispersion of traffic-related pollution. *Atmospheric*
478 *Environment*, **43**, 5101-5111.
- 479 Held, T., D. P. Y. Chang, D. A. Niemeier, 2003: UCD 2001: an improved model to simulate
480 pollutant dispersion from roadways. *Atmospheric Environment*, **37**, 5325-5336.
- 481 Hertel, O., R. Berkowicz, 1989: Operational Street Pollution Model (OSPM). Evaluation of
482 the model on data from St. Olavs street in Oslo. *DMU Luft A-135*.
- 483 Krewski, D., Jerrett, M., Burnett, R. T., MA, R., Hughes, E., Shi, Y., Turner, M. C., Pope III,
484 C. A., Thurston, G., Calle, E. E., 2009: *Extended follow-up and spatial analysis of the*
485 *American Cancer Society study linking particulate air pollution and mortality*. Health
486 Effects Institute Cambridge, MA, USA.
- 487 McCreanor, J., Cullinan, P., Nieuwenhuijsen, M. J., Stewart-Evans, J., Malliarou, E., Jarup,
488 L., Harrington, R., Svartengren, M., Han, I.-K., Ohman-Strickland, P., Chung, K. F.,
489 Zhang, J., 2007: Respiratory Effects of Exposure to Diesel Traffic in Persons with
490 Asthma. *New England Journal of Medicine*, **357**, 2348-2358.
- 491 McHugh, C. A., D. J. Carruthers, H. A. Edmunds, 1997: ADMS-Urban: an air quality
492 management system for traffic, domestic and industrial pollution. *International Journal of*
493 *Environment and Pollution*, **8**, 666-674.
- 494 Pearson, R. L., H. Wachtel, K. L. Ebi, 2000: Distance-Weighted Traffic Density in Proximity
495 to a Home Is a Risk Factor for Leukemia and Other Childhood Cancers. *Journal of the*
496 *Air & Waste Management Association*, **50**, 175-180.
- 497 Peters, A., S. von Klot, M. Heier, I. Trentinaglia, A. Hörmann, H. E. Wichmann, H. Löwel,
498 2004: Exposure to Traffic and the Onset of Myocardial Infarction. *New England Journal*
499 *of Medicine*, **351**, 1721-1730.
- 500 Petersen, W., 1980: User's guide for HIWAY-2, a highway air pollution model, EPA-600/8-
501 80-018.
- 502 Press, W. H., B. P. Flannery, S. A. Teukolsky, W. T. Vetterling, 1992: *Numerical Recipes in*
503 *FORTRAN: the art of scientific computing*. 2nd ed. Cambridge University Press.
- 504 Qian, W., A. Venkatram, 2011: Performance of Steady-State Dispersion Models Under Low
505 Wind-Speed Conditions. *Boundary-Layer Meteorology*, **138**, 475-491.
- 506 Riediker, M., Cascio, W. E., Griggs, T. R., Herbst, M. C., Bromberg, P. A., Neas, L.,
507 Williams, R. W., Delvin, R. B., 2004: Particulate Matter Exposure in Cars Is Associated
508 with Cardiovascular Effects in Healthy Young Men. *American Journal of Respiratory and*
509 *Critical Care Medicine*, **169**, 934-940.

- 510 Taylor, G. I., 1921: Diffusion by continuous movements. *Proc. London Math. Soc., Ser. 2,*
511 *20, 196.*
- 512 Thoma, E. D., Shores, R. C., Isakov, V., Baldauf, R. W. 2008. Characterization of near-road
513 pollutant gradients using path-integrated optical remote sensing. *Journal of the Air &*
514 *Waste Management Association, 58, 879-890.*
- 515 van Ulden, A. P., 1978: Simple estimates for vertical diffusion from sources near the ground.
516 *Atmospheric Environment (1967), 12, 2125-2129.*
- 517 Venkatram, A., 1992: Vertical dispersion of ground-level releases in the surface boundary
518 layer. *Atmospheric Environment. Part A. General Topics, 26, 947-949.*
- 519 Venkatram, A., V. Isakov, E. Thoma, R. Baldauf, 2007: Analysis of air quality data near
520 roadways using a dispersion model. *Atmospheric Environment, 41, 9481-9497.*
- 521 Venkatram, A., 2008: Computing and Displaying Model Performance Statistics. *Atmospheric*
522 *Environment, 42, 6882-6868.*
- 523 Venkatram, A., M. G. Snyder, D. K. Heist, S. G. Perry, W. B. Petersen, V. Isakov, 2013: Re-
524 formulation of Plume Spread for Near-Surface Dispersion. *Atmospheric Environment*
525 *(submitted).*
- 526 Wang, Y. J., K. M. Zhang, 2009: Modeling Near-Road Air Quality Using a Computational
527 Fluid Dynamics Model, CFD-VIT-RIT. *Environmental science & technology, 43, 7778-*
528 *7783.*
- 529 Wilhelm, M., B. Ritz, February 2003: Residential Proximity to Traffic and Adverse Birth
530 Outcomes in Los Angeles County, California, 1994-1996. *Environmental Health*
531 *Perspectives, 111, 207-216.*